Published in : Steel Construction (2019), vol. 12, n°3, pp. 222–230
DOI: 10.1002/stco.201900020
Status : Postprint (Author's version)

RESISTANCE OF THE BEAM-TO-COLUMN COMPONENT "COLUMN WEB PANEL IN SHEAR"

Nominated for the Bernt Johansson Outstanding Paper Awards at Nordic Steel 2019

Adrien Corman[a], Jean-Pierre Jaspart[a], Jean-François Demonceau[a]

[a]*Université de Liège, Département ArGEnCo, Bâtiment B52/3 , Quartier Polytech 1, Allée de la Découverte 9, 4000 Liège, Belgium*

Keywords :

Steel joints, component method, column web panel in shear, FEM

Abstract

The "column web panel in shear" is known to be a key component in the design of steel and steel-concrete composite joints as it can provide a reserve of ductility at the joint when activated and appropriately designed. Therefore, its behaviour has been studied for years and was thought to have been fully understood. However, some recent research projects have demonstrated that, in many cases, the simple analytical model proposed in Eurocode 3, Part 1-8, significantly overestimates the actual resistance of this component. In this context, this paper will look at the first results of investigations into that problem conducted at Liège University. In particular, beam-to-column welded joints have been studied in order to: i) highlight the aforementioned problem through comparisons between existing experimental results and Eurocode 3 predictions, ii) develop a sophisticated finite element model using the Abaqus© software, iii) validate this FE model using existing experimental results and iv) develop an extensive parametric study in order to highlight the key parameters governing the resistance capacity of the component studied. Based on the investigations conducted, the final goal consists of providing a new analytical formulation that is able to predict more accurately the shear strength of the column web panel.

1. Introduction

This article deals with the rotational behaviour of single- or double-sided beam-to-column steel joints loaded as illustrated in **Fig. 1**. Their response may be divided into different contributions. These are illustrated in **Fig. 2**, as an example, for joints in which the beams only transfer bending moments and shear forces.

Published in : Steel Construction (2019), vol. 12, n°3, pp. 222–230
DOI: 10.1002/stco.201900020
Status : Postprint (Author's version)

- The deformation of the connection under the tensile and compressive forces F_b, statically equivalent to the moment M_b at the beam end. This includes the deformation of the connection elements (e.g. bolts, endplate, …) and that of the column web under the F_b load introduction forces and results in a relative rotation $\emptyset_c$ between the beam and column axes, which makes it possible to establish a first deformation curve $M_b - \emptyset_c$ [1]. It may generally be assumed that the shear force does not affect the rotational response of the connection significantly.
- The deformation of the column web panel in shear under the combination of the couple of forces F_b and the shear forces V_c in the column at the level of the beam flanges. This shear force V_{wp}, which may be evaluated with **Eq. (1)** below, results in a relative rotation γ between the beam and column axes, thus leading to a second deformation curve $V_{wp} - \gamma$. In view of a simplified modelling of the joints for structural analysis, it is sometimes suggested to substitute a $M_p - \gamma$ curve for the $V_{wp} - \gamma$ curve through the use of a so-called transformation parameter β defined by **Eq. (1)**, see [1].

$$V_{wp} = \frac{M_{b1} - M_{b2}}{h} - \frac{V_{c1} - V_{c2}}{2} = \frac{F_b}{\beta} \qquad (1)$$

where:

β transformation parameter

h lever arm between centres of tension and compression

The present paper focuses on the behaviour of the column web panel (CWP), which together with the surrounding elements (i.e. stiffeners, column flanges, root fillets, …) forms the so-called panel zone (PZ). This zone turns out to govern the joint resistance in a significant number of situations under static loads, but even more so under seismic loading conditions. Part 1-8 of Eurocode 3 ([3]) proposes a simple trilinear analytical model to predict the behaviour of the PZ in terms of shear resistance vs. shear distortion γ of the PZ, as depicted in **Fig. 3**. This model features an elastic branch up to the elastic shear resistance of the PZ, then an elasto-plastic branch to reach the plastic shear resistance of the PZ (i.e. $V_{PZ,Rk,EC3}$) and, finally, a plateau. The elastic stiffness $K_{e,PZ}$ is given by **Eq. (2)**. The elastic shear resistance of the PZ may be assumed to be equal to two-thirds of $V_{PZ,Rk,EC3}$. The value of $V_{PZ,Rk,EC3}$ is given by **Eq. (3)** and can be divided into the contribution of the CWP (see **Eq. (4)**) and that of the surrounding elements (see **Eq. (5)**). However, the latter may only be taken into account in the presence of transverse column web stiffeners that are aligned with the beam flanges and which, together with the column flanges, form a resisting frame. Finally, it is assumed that the level of deformation associated with $V_{PZ,Rk,EC3}$ is proportional to $\frac{K_{e,PZ}}{3}$.

$$K_{e,PZ} = \frac{E}{2 \cdot (1+\upsilon)} \cdot A_{VC} \qquad (2)$$

$$V_{PZ,Rk,EC3} = V_{y,Rk,EC3} + \Delta Y_{y,Rk,EC3} \qquad (3)$$

Published in : Steel Construction (2019), vol. 12, n°3, pp. 222–230
DOI: 10.1002/stco.201900020
Status : Postprint (Author's version)

with:

$$V_{\mathrm{y,Rk,EC3}} = \rho \cdot \frac{f_{\mathrm{y,wc}}}{\sqrt{3}} \cdot A_{\mathrm{VC}} \qquad (4)$$

$$\Delta V_{\mathrm{y,Rk,EC3}} = \begin{cases} 0 \text{ if no transverse column web stiffeners are used} \\ 4 \cdot \frac{M_{\mathrm{pl,fc,Rk}}}{d_s} \text{ if transverse column web stiffeners are used} \end{cases} \qquad (5)$$

where:

E Young's modulus

A_{VC} shear area of column defined in [4]

P a reduction factor to take account of the stress interaction within the CWP (equal to 0.9)

$f_{\mathrm{y,wc}}$ characteristic yield strength of steel

$M_{\mathrm{pl,fc,Rk}}$ characteristic plastic moment resistance of a column flange

d_s distance between centrelines of stiffeners

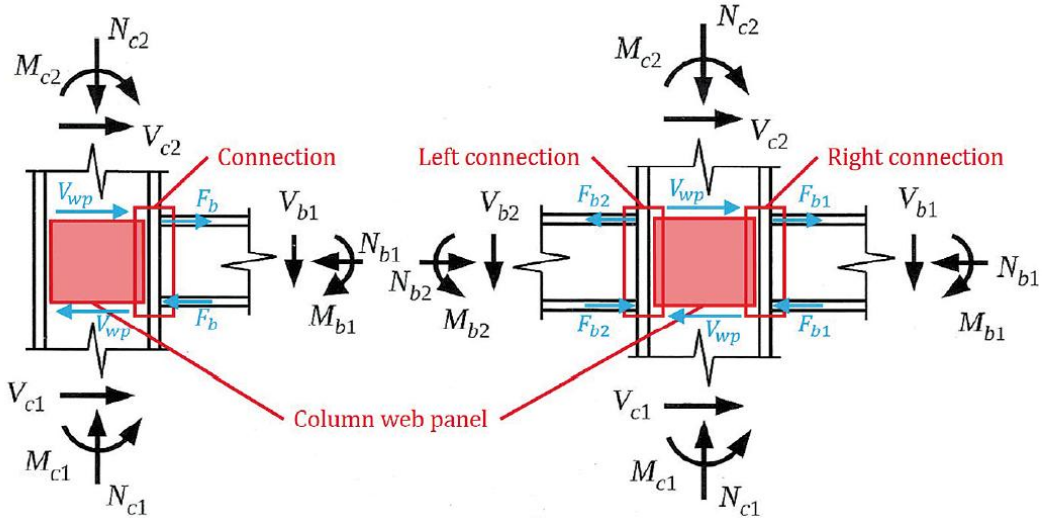

Fig. 1. Single- and double-sided joint configurations (adapted from [1])

Published in : Steel Construction (2019), vol. 12, n°3, pp. 222–230
DOI: 10.1002/stco.201900020
Status : Postprint (Author's version)

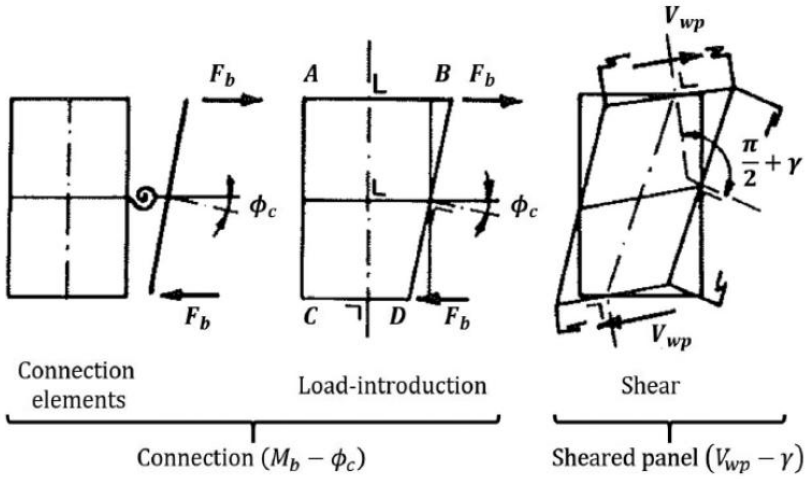

Fig. 2. Joint deformability sources (adapted from [2])

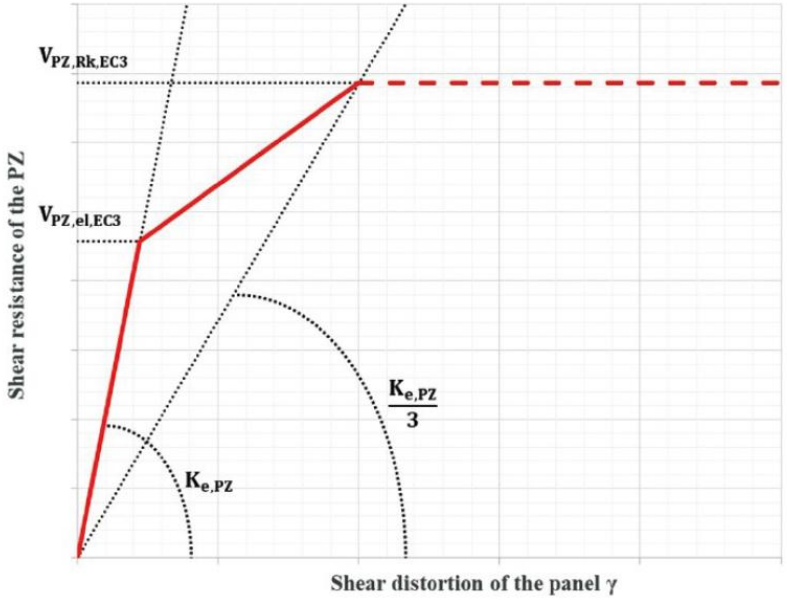

Fig. 3. EC3 trilinear model

2. Comparison with experimental results and conclusions

First of all, EC3 prediction formulae were compared with a wide range of experimental results from the scientific literature ([5]–[8]) in order to highlight potential inconsistencies in the analytical model. The experimental tests differ according the type of connection being used (welded vs. bolted) as well as the presence or otherwise of transverse column web stiffeners, and all are characterized by a web panel failure mode. **Fig. 4** illustrates the results of the comparisons for one test per experimental campaign.

The results are presented in terms of moment-rotation curves, the rotation being either the shear distortion γ of the CWP or the total rotation of the joint when the former is not available. Therefore,

Published in : Steel Construction (2019), vol. 12, n°3, pp. 222–230
DOI: 10.1002/stco.201900020
Status : Postprint (Author's version)

the EC3 trilinear model introduced in section 1 above in terms of a $V_{Rk} - \gamma$ curve had to be transformed into a $F_{Rk} - \gamma$ curve through the use of the transformation parameter β (see **Eq. (1)**), and then to a $M_{Rk} - \gamma$ curve by multiplying the resisting force F_{Rk} by the lever arm (see the solid lines in red in **Fig. 4**). The goal of the paper being to assess the accuracy of the EC3 formula for the plastic shear resistance $M_{pl,EC3}$, it was also necessary to define the experimental plastic resistance $M_{pl,exp}$. This was defined similarly to $M_{pl,EC3}$ as the intersection between the experimental curve and the straight line starting from the origin of the graph and characterized by a stiffness equal to one-third of the elastic stiffness.

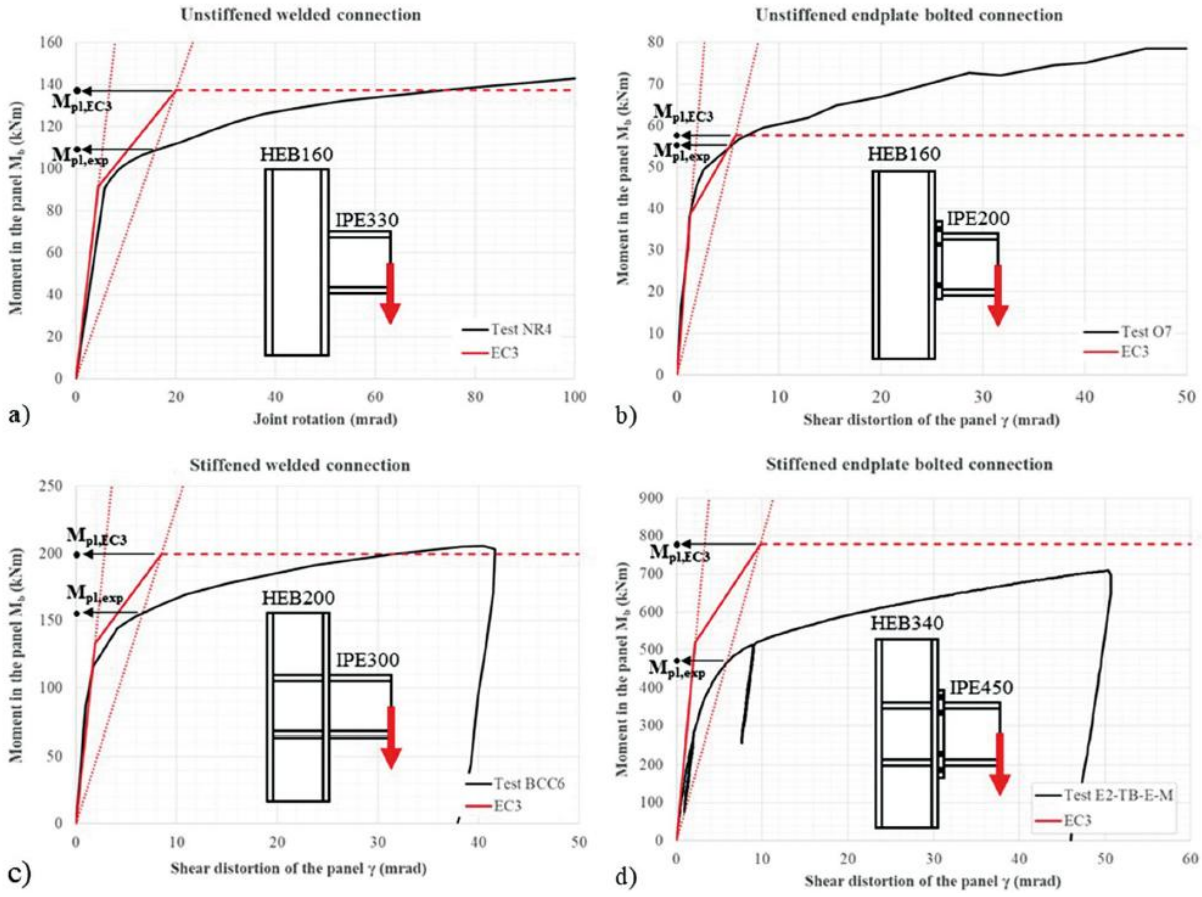

Fig. 4. Comparison between experimental results and trilinear EC3 predictions: a) test NR4 [5], b) test 07 [6], c) test BCC6 [7], d) test E2-TB-E-M [8]

Two general conclusions can be drawn from **Fig. 4**, which seem valid whatever the type of connection:

- Good agreement is observed between EC3 predictions and experimental results in terms of initial stiffness.
- By contrast, a significant discrepancy may appear as far as plastic resistance is concerned, EC3 predictions often overestimating (**Fig. 4**a, **Fig. 4**c and **Fig. 4**d) the actual shear plastic resistance of the PZ.

These observations show that **Eqs. (3)**, **(4)** and **(5)** need to be improved, whereas **Eq. (2)** may be left unchanged.

Published in : Steel Construction (2019), vol. 12, n°3, pp. 222–230
DOI: 10.1002/stco.201900020
Status : Postprint (Author's version)

3. Development of an FE model and validation

In order to investigate further the conclusions thus drawn, a numerical model was built using the commercial finite element software Abaqus© and validated against available experimental data. Configurations NR4 and NR16, taken from [5], were selected for the purpose of validation. Those two configurations consist of an IPE330 beam welded to an HEB160 column and an HEB500 beam welded to an HEB300 column respectively. All actual geometrical data may be found in [5].

The choice of these two joints is not meaningless as they had already been numerically modelled in [9] using the FINELG© software. Therefore, material laws were taken directly from [9]. Moreover, fillet welds were not modelled explicitly, although an initial geometrical imperfection was taken into account similarly to [9]. The magnitude of the initial imperfection was fixed at "d/200", where d is the clear depth of the column.

A major difference between the studies carried out by means of FINELG© and Abaqus© concerns the type of element used: shell elements in [9] and brick elements in the present study. This is due to the fact that the root fillets of the column section are believed to play a significant role in the behaviour of the CWP and therefore have to be modelled properly – something that is not possible with shell elements. Nevertheless, eight-node linear bricks with reduced integration (C3D8R elements) were used for almost all the elements except for the root fillets, which were modelled using six-node triangular prisms with full integration (C3D6 elements). **Fig. 5**a gives a general overview of the final mesh. Both mesh density and finite element type were selected based on a preliminary sensitivity analysis.

A monotonic displacement history was imposed on the beam tip in order to mimic the real loading conditions. Furthermore, the beam end section was properly restrained against out-of-plane displacement. Numerical simulations were performed using a general static analysis.

The model was validated through comparisons between experimental and numerical results in terms of force vs. vertical displacement at the beam tip, as shown in **Fig. 5**b. The following conclusions may be drawn from those comparisons and are valid for both configurations, NR4 and NR16:

- The initial stiffness in the numerical model is significantly larger than the experimental one, whereas the level of plastic resistance seems to be appropriately captured by the numerical model.
- This initial stiffness discrepancy can be explained by the initial flexibility of the test setup, which was not measured and therefore not taken into account in the numerical model.
- In order to compensate for this effect, the elastic contribution of the test setup to the measured deformations of the specimen was estimated and removed from the experimental curves (see "modified experimental curves" in Fig. 5b).
- By doing this it becomes clearer that the numerical results fit the experimental ones in terms of plastic resistance.
- The second part of the curve is overestimated by Abaqus©. This is due to the fact that strain hardening properties as well as ultimate strength were not made available in [5] and therefore

Published in : Steel Construction (2019), vol. 12, n°3, pp. 222–230
DOI: 10.1002/stco.201900020
Status : Postprint (Author's version)

had to be assumed in [9]. However, again, this is not of much concern as it is only the first part of the curve that is being investigated in this study.

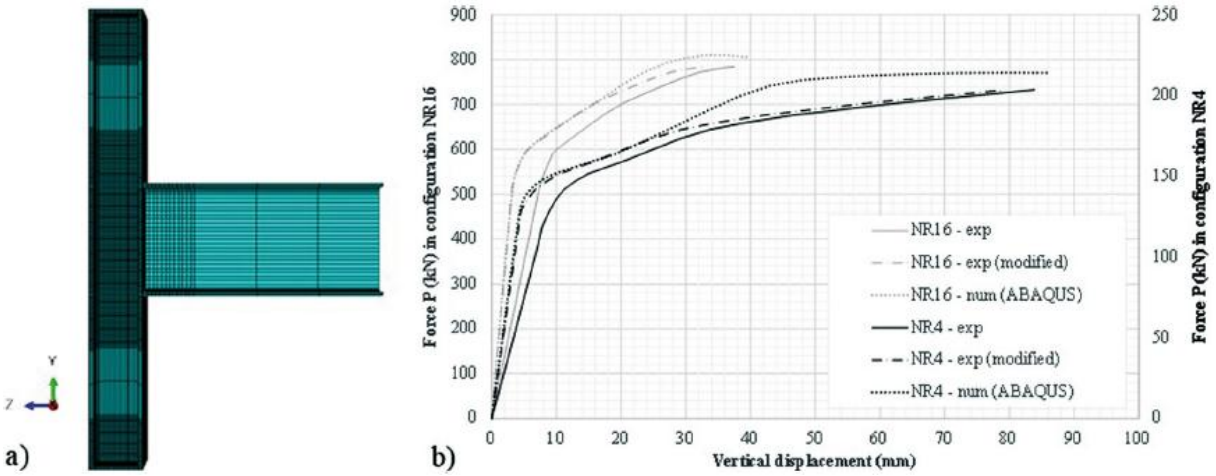

Fig. 5. Finite element modelling: a) meshed model, b) validation of numerical model

4. Parametric study

The effect of three parameters was investigated within the scope of the present study. Those parameters are listed in **Table 1**, which also provides a general overview of the different numerical simulations that were performed. The objective of the numerical study was to appraise the influence of those parameters on the plastic shear resistance of the PZ. This can be done by studying and understanding physically in Abaqus© how the stresses flow across the panel and the surrounding elements as well as how yielding spreads inside the panel.

Table 1. General overview of numerical simulations.

Configuration	Transverse column web stiffeners	Simulation of root fillets in column	Type of joint	Test numbers	Loading situation
X stands for 4 or 16	*Yes ..... 1* *No 0*	*Yes ..... 1* *No 0*	*Single-sided ..... s* *Double-sided ..... d*		
NRX	1	1	s	NRX-1-1-s	
		0		NRX-1-0-s	
		1	d	NRX-1-1-d	
		0		NRX-1-0-d	
	0	1	s	NRX-0-1-s	
		0		NRX-0-0-s	
		1	d	NRX-0-1-d	
		0		NRX-0-0-d	

Published in : Steel Construction (2019), vol. 12, n°3, pp. 222–230
DOI: 10.1002/stco.201900020
Status : Postprint (Author's version)

The following assumptions were made with the aim of isolating the behaviour of the PZ:

- The parametric study was performed on welded connections only in order to reduce the interactions with other components (e.g. bolts in tension, endplate in bending, …).
- The beam web was first disconnected from the column flange in order to fix once and for all the value of the lever arm between the centres of tension and compression in **Eq. (1)** equal to the distance between the beam flanges. Obviously, this does not reflect the reality and so the difference between "flanges welded" and "flanges and web" welded situations will be discussed at the end of this section.
- An elastic-perfectly plastic law (i.e. strain hardening neglected) was assumed for the column steel material to facilitate the derivation of the plastic resistance of the PZ.
- It was assumed that the steel in the beam section follows a linear elastic law indefinitely in order to prevent the occurrence of any failure mode (i.e. local buckling or yielding) in the beam flanges prior to the yielding of the PZ.

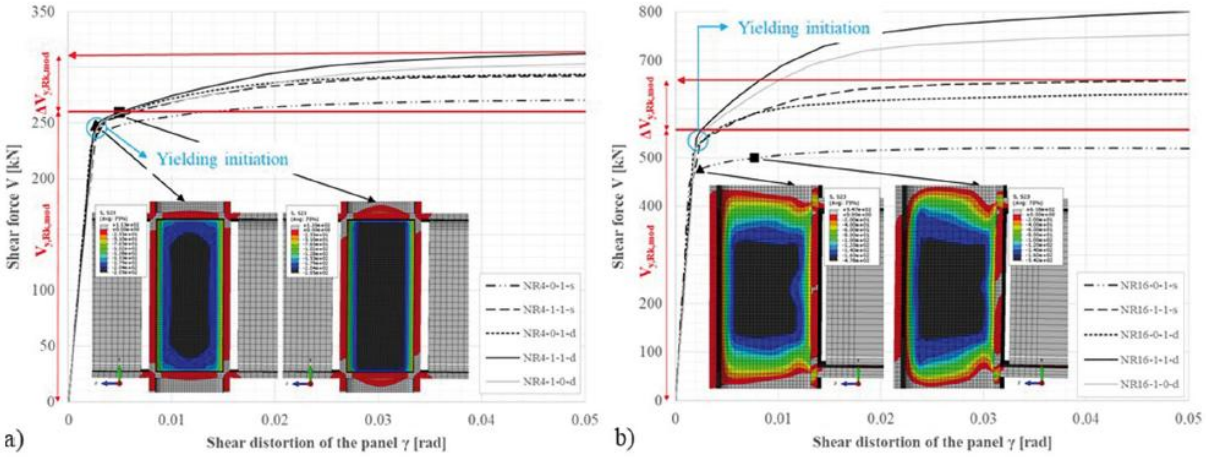

Fig. 6. $V_{wp} - \gamma$ curves: a) configuration NR4, b) configuration NR16

The results of the parametric study are depicted in **Fig. 6** in terms of shear force vs. shear distortion in the CWP. The influence of the different parameters is discussed below:

- Neither the type of joint (i.e. single- vs. double-sided) nor the presence of transverse column web stiffeners affects the initial stiffness, this observation being in line with the conclusions derived in section 2.
- Yielding initiates in the centre of the CWP and is not affected by surrounding elements. This is due to the fact that the stiffness of the CWP in shear is significantly larger than that of the surrounding elements, and so the CWP first "attracts" most of the forces.
- Yielding very quickly spreads across the entire panel, as depicted in **Fig. 6**a. The plastic resistance of the CWP is reached for a $V_{y,Rk,mod}$ value. Extra shear forces are then transferred to the surrounding elements, which most of the time contribute to the resistance of the PZ with a $\Delta V_{y,Rk,mod}$ value before large plastic rotations develop. These two contributions are clearly highlighted in red in **Fig. 6**a and **Fig. 6**b for two particular configurations (i.e. NR4-1-1-d and NR16-1-1-s). Section 5 will be dedicated to their precise quantification.

Published in : Steel Construction (2019), vol. 12, n°3, pp. 222–230
DOI: 10.1002/stco.201900020
Status : Postprint (Author's version)

– For unstiffened single-sided configurations, initiation of yielding occurs earlier because of strong stresses interacting at the level of the beam flanges, where loads are introduced into the PZ. Furthermore, the contribution of the surrounding elements remains very low with respect to the resistance of the CWP (see **Fig. 6**b).

These conclusions have been derived for particular joints where the beam web has been disconnected from the column flange. In classical welded joints (see **Fig. 7**a), loads are introduced into the CWP over its whole height, subsequently leading to a parabolic distribution of shear forces in the column web. In order to define the equivalent lever arm h_{eq} between the resulting tension and compression forces, the exact location of the centres of tension and compression is required, but is complex to derive in practice. Therefore, it was decided to disconnect the beam web from the column flange, as shown in **Fig. 7**b. By proceeding like this, the distribution of shear force in the CWP is constant and known. Centres of tension and compression are located in the beam flanges and the lever arm is known and equal to the distance d_s between the centrelines of the stiffeners. The influence of this parameter was studied for one particular case, namely, configuration NR16-1-1-s (see **Fig. 7**c). Results are presented in terms of force vs. vertical displacement at the beam tip and show good agreement between the two types of connection, at least until the CWP yields. A discrepancy may then be observed in terms of stiffness and resistance when the surrounding elements start playing a role, i.e. further to CWP yielding. This discrepancy may easily be explained by the fact that the column flange may deform in bending when it is not connected to the beam web. As a conclusion, for the derivation of the plastic resistance $V_{y,Rk,mod}$ of the CWP, the connection or disconnection of the web may be disregarded. By contrast, the $DV_{y,Rk,mod}$ contribution of the surrounding elements should be derived by explicitly accounting for this parameter in order to capture the actual stiffness and resistance properties further to the yielding of the CWP. But as this effect remains rather limited, the same model will be proposed here, irrespective of the fact that the beam web is or is not connected to the column.

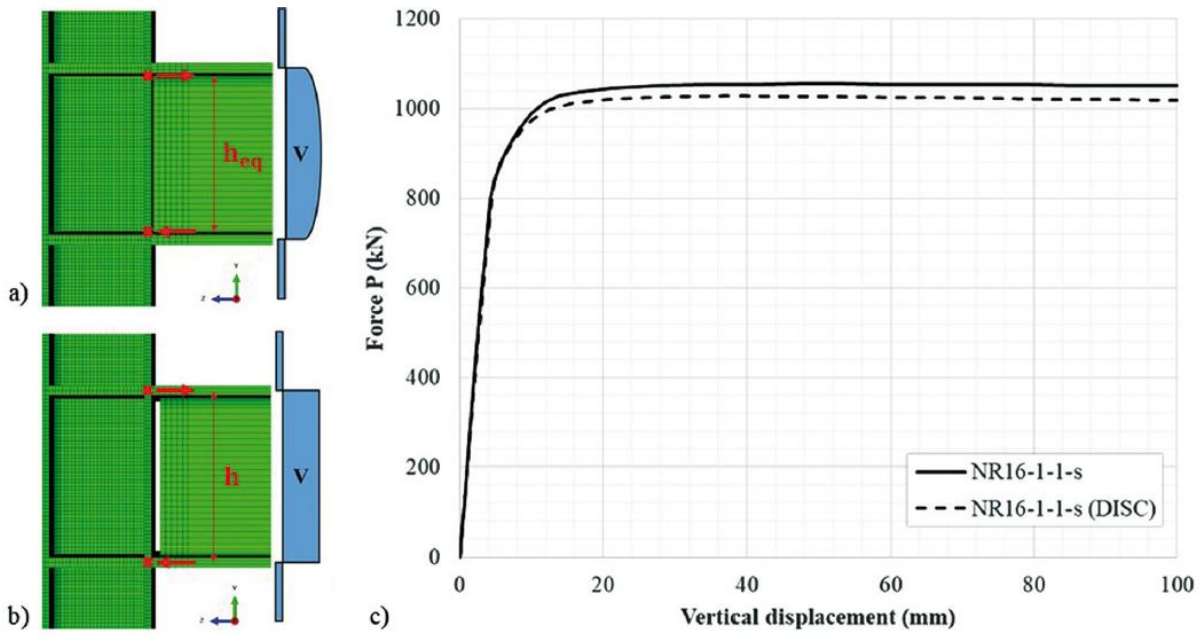

Fig. 7. Validity of the assumption for the lever arm: a) classical welded joint, b) particular welded joint where the beam web has been disconnected, c) comparison between these two joints in terms of force vs. displacement at beam tip

Published in : Steel Construction (2019), vol. 12, n°3, pp. 222–230
DOI: 10.1002/stco.201900020
Status : Postprint (Author's version)

5. Towards a mechanical model of the PZ

The conclusions drawn from section 4 clearly indicate that the behaviour of the PZ may always be divided into the contributions of the CWP ($V_{y,Rk,mod}$) and the surrounding elements ($\Delta V_{y,Rk,mod}$), as follows:

$$V_{PZ,Rk,mod} = V_{y,Rk,mod} + \Delta V_{y,Rk,mod} \quad (6)$$

This formalism is similar to **Eq. (3)**, the major difference being that both contributions need to be re-evaluated. In order to do so, it was decided to consider first unstiffened double-sided configurations to limit the influence of stress interaction in the CWP. The results are presented for configuration NR4-0-1-d but are also valid for configuration NR16-0-1-d.

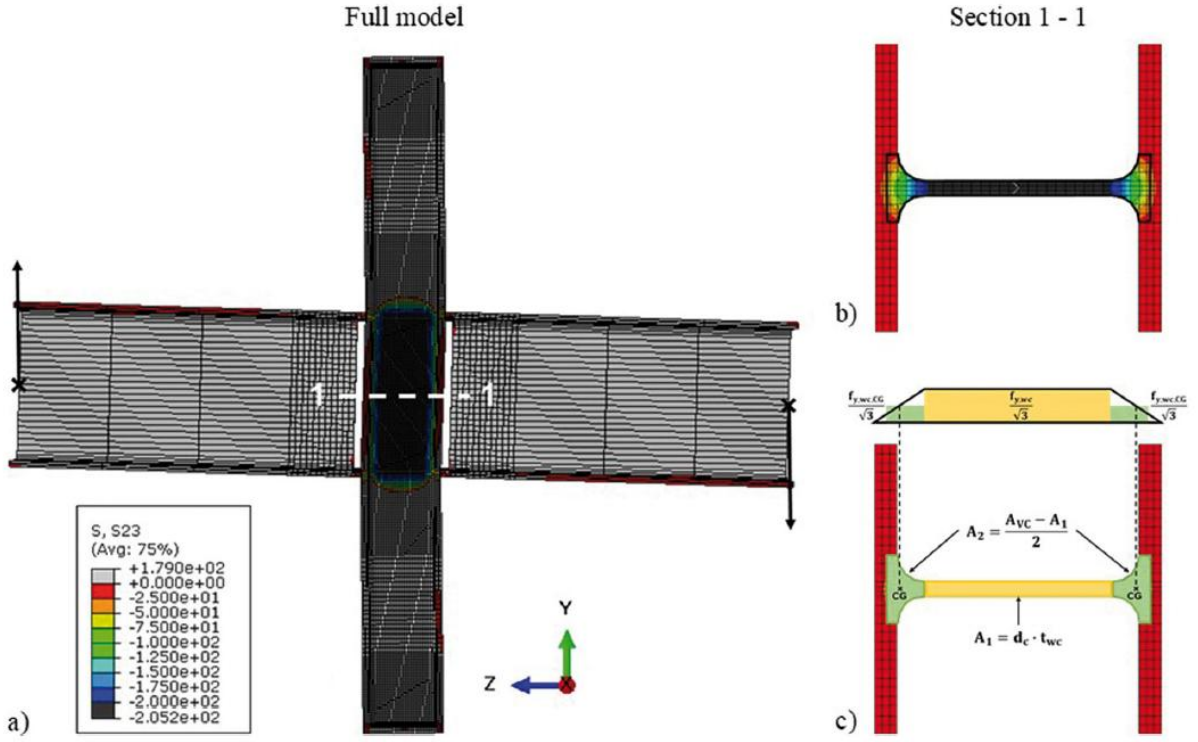

Fig. 8. Estimation of $V_{y,Rk,mod}$ contribution: a) choice of representative section, b) numerical integration, c) analytical integration

The contribution of the CWP ($V_{y,Rk,mod}$) was assessed through the use of numerical integration. To do so, the central section shown in Fig. 8a was isolated, this section being assumed to be representative of the general state of shear stress in the CWP at yielding. Shear stresses were then integrated over the area highlighted in **Fig. 8**b; the result is illustrated in **Fig. 9** (see the dotted line). This curve clearly features a plateau that corresponds to the yielding of the CWP. The distribution of shear stress at yielding (see **Fig. 8**b) clearly shows that, strictly speaking, only the clear depth of the column section yields. Therefore, a uniform distribution of shear stress may be considered over that area, as depicted by the yellow rectangles in **Fig. 8**c. Once the flow of shear stress reaches the root fillets and the flanges of the section, it spreads over a larger area, which coincides with a general decrease in the level of shear stress. As a first attempt, a linearly decreasing distribution of the shear stress, as shown in **Fig.**

Published in : Steel Construction (2019), vol. 12, n°3, pp. 222–230
DOI: 10.1002/stco.201900020
Status : Postprint (Author's version)

8c, was assumed here. This assumption made it possible to derive the level of shear stress $f_{y,wc,CG}$ at the centre of gravity of area A_2, this value being used as the mean shear stress for the whole area A_2, as depicted by the green rectangles in **Fig. 8**c. Therefore, an analytical estimation of the CWP's plastic resistance may be expressed through **Eq. (7)** as the sum of the two aforementioned contributions. This analytical prediction is plotted in **Fig. 9** (see the solid line) and shows rather good agreement with the numerical one.

$$V_{y,Rk,mod} = A_1 \cdot \frac{f_{y,wc}}{\sqrt{3}} + 2 \cdot A_2 \cdot \frac{f_{y,wc,CG}}{\sqrt{3}} \qquad (7)$$

where:

A_1 area defined in **Fig. 8**c

A_2 area defined in **Fig. 8**c

$f_{y,wc,CG}$ level of shear stress at centre of gravity of area A_2, assuming a linearly decreasing distribution of shear stress

$f_{y,wc}$ characteristic yield strength of steel

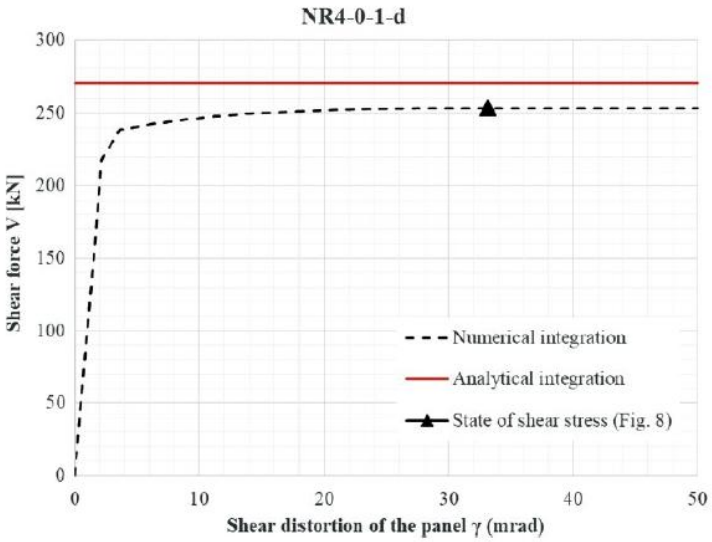

Fig. 9. Comparison between numerical and analytical estimations of $V_{y,Rk,mod}$ contribution

Beyond the yielding of the CWP, extra shear forces are transferred to the surrounding elements, i.e. to the column flanges in the case of unstiffened double-sided configurations, until a collapse mechanism develops. This collapse mechanism is activated regardless of the presence or otherwise of transverse column web stiffeners and it consists of the formation of four local hinges in the column flanges at the level of the beam flanges (see **Fig. 10**). Therefore, **Eq. (5)** may be reused to characterize the $\Delta V_{y,Rk,mod}$ contribution of the column flanges to the shear strength of the PZ (even if no transverse column web stiffeners are present and with d_s defined as the lever arm between the centres of tension and compression).

The residual stiffness that the two column flanges contribute to the system may be estimated by **Eq. (8)**. This formula corresponds to the stiffness of a rigid frame, as suggested in [10].

Published in : Steel Construction (2019), vol. 12, n°3, pp. 222–230
DOI: 10.1002/stco.201900020
Status : Postprint (Author's version)

$$K_{\mathrm{e,sur}} = 2 \cdot \frac{12 \cdot E \cdot I_{\mathrm{fc}}}{d_s^2} \qquad (8)$$

where:

I_{fc} moment of inertia of a column flange

d_{s} lever arm between centres of tension and compression

Fig. 10 provides a general overview of the evolution of the shear resistance for configuration NR4-0-1-d with respect to the level of shear distortion γ in the CWP (see the dotted line). It can be seen that the newly proposed trilinear model, which accounts for the contributions of the CWP and the surrounding elements separately, clearly yields better results than the current EC3 model, especially in terms of shear resistance, which was the purpose of this work.

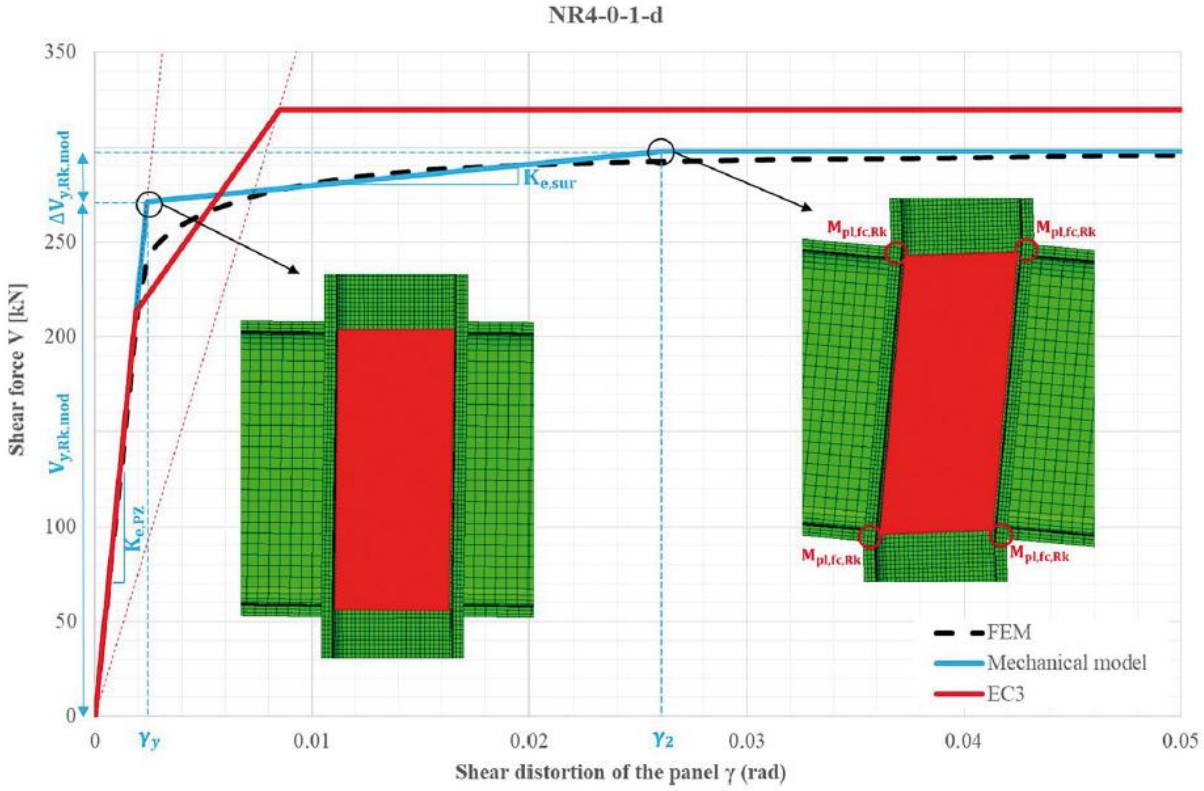

Fig. 10. Comparison of FEM results, trilinear EC3 predictions and newly proposed mechanical model

6. Conclusions and perspectives

The results clearly show that the plastic resistance of the PZ may always be divided into the contributions of the CWP ($V_{\mathrm{y,Rk,mod}}$) and the surrounding elements ($\Delta V_{\mathrm{y,Rk,mod}}$), as described by **Eq. (6)**. Therefore, it is proposed to take account of the beneficial effect provided by the surrounding elements in all cases and not only in the presence of transverse column web stiffeners, as is currently stated in EC3.

Published in : Steel Construction (2019), vol. 12, n°3, pp. 222–230
DOI: 10.1002/stco.201900020
Status : Postprint (Author's version)

Those two contributions have been quantified in this paper for the particular case of unstiffened double-sided configurations and they provide a more accurate estimation of the shear strength of the PZ than the current model proposed in EC3. Ongoing work is specifically dedicated to quantifying those two terms in the case of stiffened double-sided configurations as well as in the case of stiffened and unstiffened single-sided configurations.

For the contribution of the CWP, it also seems that a formalism similar to the one proposed in EC3 could be adopted (see **Eq. (4)**), with the major difference being that the shear area needs to be re-evaluated. This conclusion is in line with the main conclusion drawn in [11]. The definition of a simple analytical formula for the shear area requires additional work and will be reported in a future publication. The same applies to the stress interaction factor ρ in **Eq. (4)**, whose use seems relevant for single-sided joints but is much more questionable in the case of double-sided joints. Finally, an extension of the whole model to panel zones in bolted connections will have to be achieved.

References

[1] Jaspart, J.-P.; Weynand, K.: *Design of joints in steel and composite structures*. Berlin, 2016.

[2] Jaspart, J.-P.: Appendices: Recent advances in the field of steel joints: column bases and further configurations for beam-to-column joints and beam splices. Liège, 1997.

[3] European Committee for Standardization; NBN EN 19931-8 (Eurocode 3): Design of steel structures – Part 1-8: Design of joints (English version). Brussels, 2005.

[4] European Committee for Standardization: NBN EN 19931-1 (Eurocode 3) : Design of steel structures – Part 1-1: General rules and rules for buildings. Brussels, 2005.

[5] Klein, H.: Das elastisch – plastische Last-Verformungsverhalten M-theta steifenloser, geschweisster Knoten für die Berechnung von Stahlrahmen mit HEB-Stützen. Universität Innsbruck, 1985.

[6] Janss, J.; Jaspart J.-P.; Maquoi, R.: Strength and behaviour of in-plane weak axis joints and of 3-D joints, 1988, pp. 60–68.

[7] Mele, E.; Calado, L.; De Luca, A.: Experimental Investigation on European Welded Connections. *J. Struct. Eng*. **129**, 2003, No. 10, pp. 1301–1311.

[8] RFCS: EQUALJOINTS-PLUS Project under Grant Agreement No. 754048.

[9] Frey, F.; Atamaz Sibai, W.: Numerical simulation of the behaviour up to collapse of two welded unstiffened one-side flange connections. In: *Connections and the Behaviour, Strength and Design of Steel Structures*, 1987, pp. 85–92.

[10] Jaspart, J.-P. : Etude de la semi-rigidité des noeuds poutrecolonne et son influence sur la résistance et la stabilité des ossatures en acier. Liège, 1991.

[11] Brandonisio, G.; De Luca, A.; Mele, E.: Shear strength of panel zone in beam-to-column connections. *J. Constr. Steel Res*. **71**, 2012, pp. 129–142.